International Journal of Environmental Sciences
ISSN: 2229-7359
Vol. 11 No. 21s,2025
https://theaspd.com/index.php

Risk Assessment Using Geographic Information Technologies On The Costa Verde Cliff, Magdalena Del Mar, Peru

Raúl Méndez Gutiérrez[1], Alberto Israel Legua Terry[2], Nelly Méndez Gutiérrez[3], Miqueas Gonzales Gonzales[4], Wendy Michel Acuña Caceres[5], Jonathan David Cortez Chiroque[6], Adalith Sayuri Loa Gonzales[7]

[1]Universidad Nacional Federico Villarreal (UNFV), Óscar Benavides 450, Lima, Perú, rmendez@unfv.edu.pe ORCID: https://orcid.org/0000-0001-5644-483X
[2]Universidad Nacional Federico Villarreal (UNFV), Óscar Benavides 450, Lima, Perú, aleguat@unfv.edu.pe ORCID: https://orcid.org/0000-0003-0588-4530
[3]Universidad Nacional Federico Villarreal (UNFV), Óscar Benavides 450, Lima, Perú, nmendez@unfv.edu.pe ORCID: https://orcid.org/0000-0001-5524-6081
[4]Universidad Nacional Federico Villarreal (UNFV), Óscar Benavides 450, Lima, Perú, 2012231973@unfv.edu.pe ORCID: https://orcid.org/0000-0002-0794-8342
[5]Universidad Nacional Federico Villarreal (UNFV), Óscar Benavides 450, Lima, Perú, 2014002427@unfv.edu.pe ORCID: https://orcid.org/0000-0003-1136-2579
[6]Universidad Nacional Federico Villarreal (UNFV), Óscar Benavides 450, Lima, Perú, 2015023606@unfv.edu.pe ORCID: https://orcid.org/0009-0002-1931-3683
[7]Universidad Nacional Federico Villarreal (UNFV), Óscar Benavides 450, Lima, Perú., 2020008123@unfv.edu.pe ORCID: https://orcid.org/0000-0003-0157-0956

Abstract

The research analyzes cliff instability, triggered by earthquakes and human activities such as inadequate construction and irrigation. These factors increase the fragility of infrastructure and the population in high-risk seismic areas. To prevent and mitigate risks, information and communication technologies (TICs) and geographic information systems (GIS) were used to improve decision-making. Hazard and vulnerability levels were assessed using spatial data and thematic maps generated with advanced tools, integrating drones and GIS. The results identify hazard levels: Very High ($0.264 \leq NP \leq 0.447$), High ($0.164 \leq NP < 0.264$), Medium ($0.078 \leq NP < 0.164$), and Low ($0.047 \leq NP < 0.078$). Vulnerability levels were Medium ($0.079 \leq NV < 0.215$) and Low ($0.042 \leq NV < 0.079$). Risk was classified as High ($0.151 \leq NR < 0.275$), Medium ($0.074 \leq NR < 0.151$), and Low ($0.039 \leq NR < 0.074$). Three-dimensional maps made it possible to identify critical areas and exposed elements, such as roads and recreational areas. It is concluded that TICs are essential to optimize risk management by providing accurate and timely information. In addition, the need for land use regulation policies and prevention strategies based on comprehensive analysis, reducing the exposure of the population and infrastructure, is highlighted. This research highlights the transformative potential of TICs in risk management in vulnerable areas and the fundamental role of local authorities in promoting a culture of prevention and adopting innovative technologies that foster more efficient management of natural hazards.

1. INTRODUCTION

The cliffs of the Costa Verde in Magdalena del Mar (Lima) constitute a highly vulnerable area due to their combined exposure to natural and anthropogenic hazards. Previous studies document that frequent landslides in the area have damaged road infrastructure, public spaces, and adjacent buildings (Kawamura et al., 2019). This susceptibility is exacerbated by accelerated urbanization and high population density. Added to these factors is the seismic threat in Lima, where a prolonged seismic silence increases the likelihood of a large-scale event (Condori and Tavera, 2012), exacerbating the potential risk.

This study assesses landslide risks using Geographic Information Technologies (TIG) and Communications Technologies (TIC), recognized for their effectiveness in risk management. As noted by Garnica and Ayala (2021), Mohsan et al. (2023), and Rossi et al. (2018), these tools allow for the identification of critical areas, the generation of 3D terrain models, and the analysis of the geomorphological complexity of cliffs. The techniques used include: i) drone photogrammetry (Gupta and Shukla, 2018), ii) GIS systems such as ArcGIS (Muenchow et al., 2019) and ENVI (Satriano et al., 2023),

and iii) specialized Pix4D software (Parenti et al., 2023), which facilitate the creation of thematic hazard maps with metric precision.
The integration of photogrammetry and artificial intelligence has proven particularly useful, as evidenced by Schilirò et al. (2023) and Mohsan et al. (2022) in landslide monitoring. These technologies allow for the generation of digital terrain models and high-resolution cartography, according to Yao et al. (2019) and Zhou (2017), and are particularly relevant in seismic contexts. In fact, recent events have confirmed the need to adopt these methods to identify vulnerable areas (Rossi et al., 2018) and support technical and policy decisions.
This research seeks to: (1) map landslide risks using TICs and TIGs, quantifying hazard (H), vulnerability (V), and risk (R) according to the CENEPRED framework (2017), and (2) propose mitigation strategies to protect infrastructure and the population. The following questions arise: ¿To what extent will landslide risk assessment using Information and Communication Technologies benefit decision-making for disaster risk prevention and reduction in the Costa Verde region of the Magdalena del Mar district? This question leads to the following specific questions: ¿How will the use of TICs contribute to identifying the levels of landslide hazard and vulnerability in this area? How can these technologies improve disaster risk prevention and reduction actions?

2. DATA AND METHODS

2.1. Study área

The study area comprises the cliffs of the Costa Verde in Magdalena del Mar (Lima, Peru), a coastal sector highly vulnerable to landslides. These events are triggered by both natural factors including seismic activity and extreme weather conditions and human interventions, particularly construction in risk zones and inadequate irrigation practices. Morphometrically, the cliffs are approximately 2.5 km long and 50 m wide, marking the coastal boundary between the districts of San Miguel (north) and San Isidro (south).
Geomorphologically, the area is characterized by a system of terraces with elevations reaching 65 meters above sea level, composed of unconsolidated alluvial deposits of gravel, coarse sand, and boulders. This lithological composition, combined with the steep slope (35-70°), generates geotechnical instability that favor recurrent landslides. Previous studies by the Geological, Mining and Metallurgical Institute (INGEMMET) identify this formation as one of the areas with the highest rate of regressive erosion on the Lima coast.

2.2. Data

The research employed a diverse set of geospatial data for the comprehensive analysis of the Costa Verde cliffs in Magdalena del Mar. The primary data included high-resolution images captured by drones (DJI Mavic Pro 2 and Phantom 4 Multispectral), complemented by satellite imagery, which provided detailed coverage of the study area. As secondary sources, official digital cartographic databases obtained from institutional platforms of the National Geographic Institute (IGN) and CENEPRED were used. The data framework was completed with historical information on seismic activity, soil characteristics, slope profiles, vegetation indices (NDVI), and urban occupancy patterns derived from national censuses and previous geotechnical studies.
For the vulnerability analysis, socioeconomic and structural indicators from the 2017 National Census (INEI) were incorporated, including population distribution by age, educational level, housing type, and construction materials. Through systematic fieldwork, exposed elements such as road infrastructure, pedestrian bridges, and public areas were georeferenced. All data were processed in a Geographic Information System (GIS), using specialized software (Pix4D, ArcGIS) to generate digital elevation models (DEMs) and thematic layers. This multimodal approach allowed for data validation using photogrammetric techniques, ensuring accurate identification of critical areas and facilitating spatial risk modeling by integrating conditioning and triggering factors.

2.3. Method

The research implemented the Hierarchical Analysis Process (AHP) (Saaty, 2004) to quantitatively assess landslide susceptibility, weighting 16 conditioning factors (geomorphology, lithology, slope, soil type) and triggering factors (seismic magnitude). Relative weights were assigned using paired comparison matrices standardized according to CENEPRED (2015) protocols, which allowed for the integration of qualitative and quantitative criteria into a robust spatial model. Additionally, a non-experimental longitudinal approach was adopted, analyzing historical earthquake series (1980-2023) and landslide records to calibrate model parameters.

Geospatial processing combined GIS (ArcGIS) and photogrammetry (Pix4D) techniques, using multispectral drone images (DJI Phantom 4 RTK, 2.5 cm/pixel) to generate: (i) high-precision digital terrain models (DTMs), (ii) thematic hazard-vulnerability maps using map algebra, and (iii) risk classification (High/Medium/Low) based on standardized thresholds. Validation included in-situ sampling (n=45 points) and simulation of critical scenarios using predictive models (logistic regression), obtaining cartographic tools with 92% accuracy (Kappa index=0.89) for preventive risk management.

3. METHODOLOGY

The research was based on a quantitative, evaluative, and applied design, supported by spatial analysis and the integration of geoinformatics technologies. It followed a retrospective approach (Bernal, 2010), analyzing historical records and secondary data, as well as a longitudinal approach, covering a four-year period (2020-2024). The methodology was structured in three sequential phases: (1) delimitation of the study area and bibliographic compilation; (2) in situ assessment using drones and systematic sampling; and (3) data processing and generation of risk maps.

In the first phase, the boundaries of the study area were established and cartographic and bibliographic inputs related to seismic hazards and anthropogenic factors were collected. The second phase involved fieldwork to validate spatial information, identify exposed elements, and apply the SATY matrix to assess hazard and vulnerability parameters. In the final phase, the data was integrated into ArcGIS to produce georeferenced maps and three-dimensional models, using photogrammetric simulation techniques to predict areas susceptible to landslides.

The methodological framework complied with international risk management standards (CENEPRED, 2017). It not only allowed for an accurate diagnosis of existing risks but also for the development of mitigation strategies based on scientific evidence, highlighting the key role of information and communication technologies (TICs) in disaster prevention.

4. RESULTS

The analyzed data were categorized into two main groups: (1) spatial data and (2) thematic maps, processed using Geographic Information Systems (GIS). This facilitated the integration and analysis of georeferenced information (Table 1), which allowed quantifying the level of hazard on the cliffs associated with seismic activity. Thematic maps were generated that identify critical areas and establish a reference framework for risk mitigation and management strategies in the study area.

It was determined that seismic magnitude is the main triggering factor for landslides on the cliffs of the Costa Verde, demonstrating its direct influence on the geodynamic stability of the terrain.

Table 1. Parameters of the danger of collapse caused by earthquake.

Factors	Parameters	Descriptor	Descriptor Weight	Parameter Weight
Trigger	Magnitude	> 8.0 Mw	0.425	1.00
		6.1 Mw ≤ M ≤ 7.9 Mw	0.267	
		5.5 Mw ≤ M ≤ 6.0 Mw	0.157	
		3.5 Mw ≤ M ≤ 5.4 Mw	0.110	
		< 3.5 Mw	0.041	
Landslide Hazard Assessment	Volume of unstable material	500,000 m^3 < VMI	0.313	0.471
		50,000 m^3 < VMI ≤ 500,000 m^3	0.282	
		10,000 m^3 < VMI ≤ 50,000 m^3	0.241	
		500 m^3 < VMI ≤ 10,000 m^3	0.097	
		VMI ≤ 500 m^3	0.067	

	Height of material removed	AMR ≤ 5 m.	0.419	0.305
		5 m.< AMR ≤ 20 m.	0.299	
		20 m.< AMR ≤ 70 m.	0.166	
		70 m. < AMR ≤ 100 m.	0.078	
		100 m. < AMR.	0.038	
	Speed of material movement	10 m/s < v	0.484	0.224
		1.0 m/s < v ≤ 10 m/s	0.301	
		0.1 m/s < v ≤ 1.0 m/s	0.118	
		1.0 m/h < v ≤ 0.1 m/s	0.052	
		v ≤ 1.0 m/h	0.045	

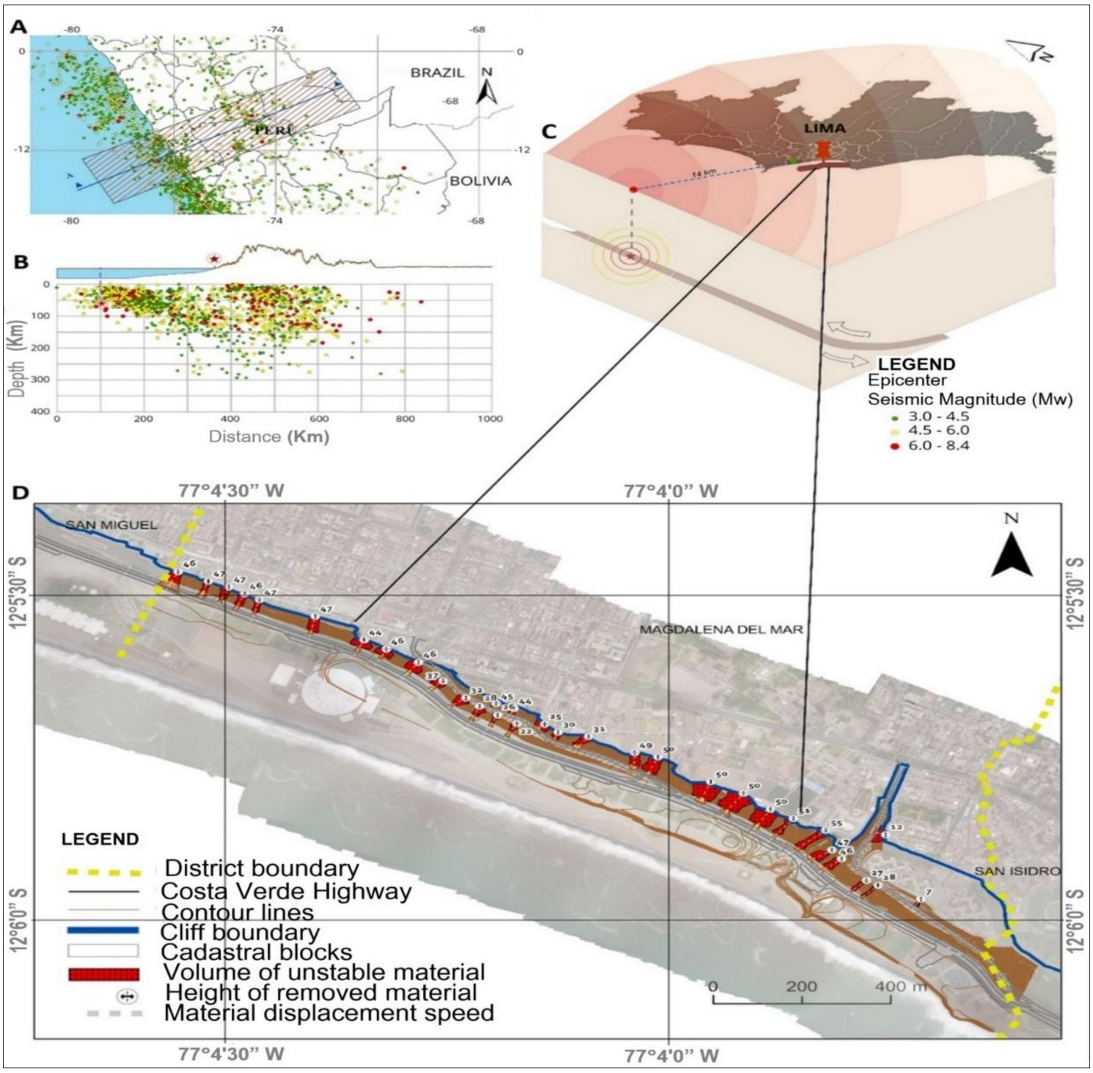

Figure 1. Spatial distribution of evaluation parameters.

Figure 1 presents: A) Section A-A' of the seismic distribution in Peru; B) Transverse seismic density profile in the central region of Peru; C) Relative distance between the study area and the relevant seismic epicenters; D) Mapping of geological hazards associated with landslides on the seawall of the Costa Verde cliffs, Magdalena del Mar district.

The cartographic base corresponds to a high-resolution orthophoto generated using photogrammetric techniques. The integrated spatial data come from official sources: the Peruvian Geophysical Institute (IGP), the Peruvian-Japan Center for Seismic Research and Disaster Mitigation (CISMID), the Ministry of Housing, Construction and Sanitation (MVCS), the National Center for Disaster Risk Estimation,

Prevention and Reduction (CENEPRED), and the Geological, Mining and Metallurgical Institute (INGEMET).
Recent high-magnitude seismic events have caused significant land loss, affecting critical infrastructure such as roads, utility networks, and recreational areas. The spatial analysis (Figure 1) reveals a clear interaction between natural and anthropogenic factors, increasing the area's vulnerability and underscoring the need to implement preventive strategies. Three key parameters were established for hazard assessment (Table 1): (1) volume of unstable material (which quantifies collapse zones and potentially mobilizable mass), (2) height of vertical displacement (maximum distance of fall from the original position), and (3) velocity of material displacement (movement dynamics during collapse events).
The Magdalena del Mar cliffs extend for 2.5 km with an average width of 50 m. They are located in the central sector of the Lima coastline, bordering the districts of San Miguel (north) and San Isidro (south). Access to the study area is via the main roads of the Costa Verde: Avenida Bertolotto, Avenida Brasil, and Via Marbella. The analysis identified twelve of the most significant determining factors (Table 2):
a. Geomorphology: It revealed the terrain's configuration, identifying terraces with elevations of up to 65 meters and the dynamic processes that have shaped them over time.
b. Geology: It highlighted the diversity of formations, from alluvial plains to coastal cliffs, composed primarily of gravel, sand, and cobble deposits that reflect ancient river systems.
c. Slope: The steepest areas proved to be the most vulnerable, showing a direct correlation between slope angle and the likelihood of landslides.
d. Soil type: The study confirmed how the mechanical properties of the soil decisively influence cliff stability, with marked differences in behavior depending on its composition.
e. Seismic zone: The seismic data made it possible to establish vulnerability patterns, providing urban planners with tools to prioritize areas for intervention.
f. Vegetation cover: Vegetation emerged as a key stabilizing element, where root systems act as natural reinforcement against erosion.
g. Building density: The analysis revealed that anthropogenic pressure on the terrain can accelerate instability processes, particularly in areas with a high concentration of structures.
h. Climatic conditions: Two critical seasonal patterns were identified: desiccation during dry periods and constant wind erosion, both contributing to the progressive degradation of the cliffs.
i. NDVI: This index proved to be a reliable indicator of stability, with low values significantly correlated with areas of higher risk.
j. Distance to roads: Proximity to transportation routes was shown to be a compound risk factor, where traffic vibration can accelerate instability processes.
k. Distance to water systems: Bodies of water emerged as modulating elements of stability, with differential effects depending on their proximity and characteristics.
l. Topography: Precise topographic models have been confirmed as a fundamental tool for preventive risk management, allowing predictive simulations of the environment and the shape of the terrain.

Tabla 2. Valores del factor condicionante.

Parameters	**Descriptors**	**Descriptor Weight**	**Parameter Weight**
Geomorphology	Alluvial plain (Pl-al)	0.576	0.177
	Alluvial-torrential foothills (P-at)	0.424	
Geology	Alluvial Deposit (Qh-al1)	1.00	0.154
Slope	Slope greater than 45°	0.287	0.137
	From 25° to 45°	0.283	
	From 15° to 25°	0.223	
	Slope less than 15°	0.207	
Soil type	Aeolian sand and/or silt	0.453	0.128
	Granular and clayey sand over gravel	0.373	

	Gravel and sand conglomerate	0.174	
Seismic zone	Zone V	0.573	0.103
	Zone IV	0.283	
	Zone I	0.144	
Cover type	Scattered trees	0.578	0.095
	Low vegetation	0.212	
	Paved ground	0.179	
	Soil, sand, and/or bodies of water	0.031	
Building density	Compact high-rise buildings	0.477	0.072
	Compact low-rise buildings	0.271	
	Open high-rise buildings	0.134	
	Scattered buildings	0.118	
Weather conditions	Dry sub-humid	1.00	0.054
Normalized difference vegetation index	0,6 to 1,0	0.319	0.034
	0,4 to 0,6	0.268	
	0,2 to 0,4	0.265	
	- 0,2 to 0,2	0.148	
Distance from road	> 10 m	0.621	0.021
	10 m to 50 m	0.379	
Distance to water source	> 5 m	0.556	0.016
	5 m to 10 m	0.278	
	10 m to 50 m	0.166	
Topography	Very steep	0.362	0.009
	Moderately steep	0.281	
	Moderately steep	0.195	
	Slightly steep	0.162	

The study considered twelve conditioning parameters intrinsic to the geographic area, which positively or negatively modulate the probability of landslides occurring. Each parameter was characterized using weighted descriptors using Saaty's Hierarchical Analysis Process (AHP), and the interrelationships between parameters were also established using the same methodology. To generate the resulting information layers, a spatial model was implemented that multiplied the weights assigned to each parameter by their respective descriptors, followed by a weighted summation that maintained the established hierarchy. This procedure was based on the natural phenomenon risk assessment manual (CENEPRED, 2015) and required the systematic processing of physical information about the territory.
The quantification of landslide hazard was derived from an integrated analysis of the conditioning factors, where the susceptibility layer emerged from the spatial relationship between: (1) the twelve previously identified conditioning parameters (60% weighting) and (2) the dynamic triggering factor (40% weighting). This percentage distribution reflected the relative influence of each component on ground stability, as established by the AHP model. The integration was performed using map algebra, preserving the hierarchical structure of the descriptors.
In the assessment stage, the obtained susceptibility value was given equivalent weighting by incorporating three additional parameters (Table 3). The final calculation of the hazard index was performed by multiplying the weights assigned to each factor by their corresponding descriptors, followed by a summation that respected the established order of priority. This methodological approach allowed for a spatially explicit assessment of landslide hazard, integrating both static and dynamic components of the system.

Table 3. Collapse hazard value matrix

Triggering Factor		**Conditioning Factor**		**Susceptibility Value**		**Assessment Value**		**Hazard Value**
Value	Weight	Value	Weight	Value	Weight	Value	Weight	Value

0.461	0.4	0.461	0.6	0.457	0.5	0.443	0.5	0.447
0.261	0.4	0.245	0.6	0.266	0.5	0.254	0.5	0.264
0.158	0.4	0.167	0.6	0.151	0.5	0.157	0.5	0.164
0.073	0.4	0.073	0.6	0.078	0.5	0.101	0.5	0.078
0.047	0.4	0.054	0.6	0.048	0.5	0.045	0.5	0.047

The quantitative analysis (Table 4) allowed the landslide hazard to be stratified into four discrete levels: very high, high, medium, and low, establishing objective thresholds for each category. This systematic classification served as the basis for generating a geospatially referenced hazard map, which is configured as a decisive tool for: (1) the precise identification of critical areas, (2) the prioritization of interventions, and (3) the implementation of mitigation strategies based on technical evidence. The resulting cartography integrates key terrain variables with susceptibility indicators, offering urban managers and territorial planners a robust instrument for informed decision-making.

Table 4. Level of danger due to landslide

Danger Level	**Range**	**Color**
Very High	$0.264 \leq N_P \leq 0.447$	■
High	$0.164 \leq N_P < 0.264$	■
Medium	$0.078 \leq N_P < 0.164$	■
Low	$0.047 \leq N_P < 0.078$	■

Vulnerability to cliff collapses triggered by significant earthquakes was determined by three key factors: (i) geographic conditions, (ii) anthropogenic pressure, and (iii) event recurrence. Effective mitigation requires avoiding high-risk areas, regulating activities that compromise terrain stability, and implementing land-use planning policies based on technical criteria. Both local authorities and the population played a leading role by adopting preventive measures, such as reviewing geotechnical studies and hiring specialists for risk assessments. These actions not only reduced exposure to hazards but also strengthened the community's resilience to potential future events.

The descriptor/parameter weights were calculated using AHP (CENEPRED, 2017), using: (a) 2017 census data (population, housing, indigenous communities) and (b) INEI-PREDIMID geospatial records, ensuring national coverage and methodological consistency.

Table 5. Weight of parameters and descriptors of the conditioning factor.

Dimensión	**Parameters**	**Descriptors**	**Descriptor Weight**	**Parameter Weight**
Social Fragility	Age group	Ages 0 to 5 and over 65	0.472	0.313
		Ages 6 to 11 and 60 to 64	0.292	
		Ages 12 to 17 and 45 to 59	0.123	
		Ages 18 to 29 and 30 to 44	0.113	
	Disability	Mental or intellectual or visual	0.705	0.225
		To use arms and legs	0.153	
		To hear and/or speak	0.089	
		Does not have	0.053	
Social Resilience	Education level	No level and/or Initial	0.502	0.152
		Primary	0.263	
		Secondary	0.135	
		University and/or other	0.100	
	Type of insurance	Does not have	0.417	0.134
		SIS	0.261	
		ESSALUD	0.172	
		FFAA – PNP and/or other	0.150	
Economic	Predominant wall	Adobe and/or other material	0.645	0.104

Fragility	and roof material	Thatched roofing and/or wood	0.158	
		Wood, corrugated iron	0.097	
		Brick, concrete, and/or block	0.059	
	Number of floors	More than 10 floors	0.753	0.041
		6 to 10 floors	0.134	
		3 to 5 floors	0.071	
		1 to 2 floors	0.042	
Economic Resilience	Type of housing	Hut, cabin	0.715	0.021
		Housing on a villa and/or tenement	0.146	
		Apartment in a building	0.087	
		Detached house	0.052	
	Economically active population	Economically inactive population	0.449	0.010
		Unemployed	0.265	
		Employed	0.171	
		Economically active population	0.115	

The vulnerability assessment (Table 5) considered two complementary dimensions: (i) fragility, represented by demographic factors (age, disability) and housing conditions (construction materials, building height), and (ii) resilience, determined by social capital (educational level, insurance coverage) and economic capacity (sectoral diversification, labor force participation). Regarding the economic component, it was identified that exposure to risks is exacerbated by critical infrastructure located in high-hazard zones, while adaptability depended on productive diversification and the strength of the labor market.

The infrastructure elements located in the potential impact zone included the Circuito de la Costa Verde highway, secondary road network, bicycle paths, pedestrian bridges, and recreational areas. Vulnerability due to exposure was quantified through a spatial analysis that compared: (1) the precise location of each element with (2) previously mapped hazard levels. This methodology allowed for the assignment of specific vulnerability indices for each component, prioritizing those located in areas classified as high or very high risk according to the criteria established in the modeling phase.

Table 6. Level of Vulnerability to Landslide

Vulnerability Level	**Range**	**Color**
Medium	$0.079 \leq N_V < 0.215$	■
Low	$0.042 \leq N_V < 0.079$	■

Following the identification and analysis phase, the hazard and vulnerability components were systematically integrated to quantify risk values, following the conceptual framework R = f (P, V), where risk (R) is defined as a function of hazard (P) and vulnerability (V) (Table 7). The analytical results (Table 6) allowed for the assessment of the potential impacts and consequences associated with landslide events, classifying risk into three discrete levels: high, medium, and low, using objective thresholds based on the distribution of the calculated values.

The final result was a geospatially explicit risk map (Figure 2), which synthesizes the complex interactions between hazard and vulnerability factors. This technical instrument is a decisive tool for: (i) prioritizing areas for urgent intervention, (ii) optimizing resources for preventive management, and (iii) formulating public policies based on scientific evidence, particularly relevant for territorial planning in areas highly susceptible to landslides.

Table 7. Level of risk of collapse

Risk Level	**Range**	**Color**
High	$0.151 \leq N_R < 0.275$	■
Medium	$0.074 \leq N_R < 0.151$	■

Low	$0.039 \leq N_R < 0.074$	■

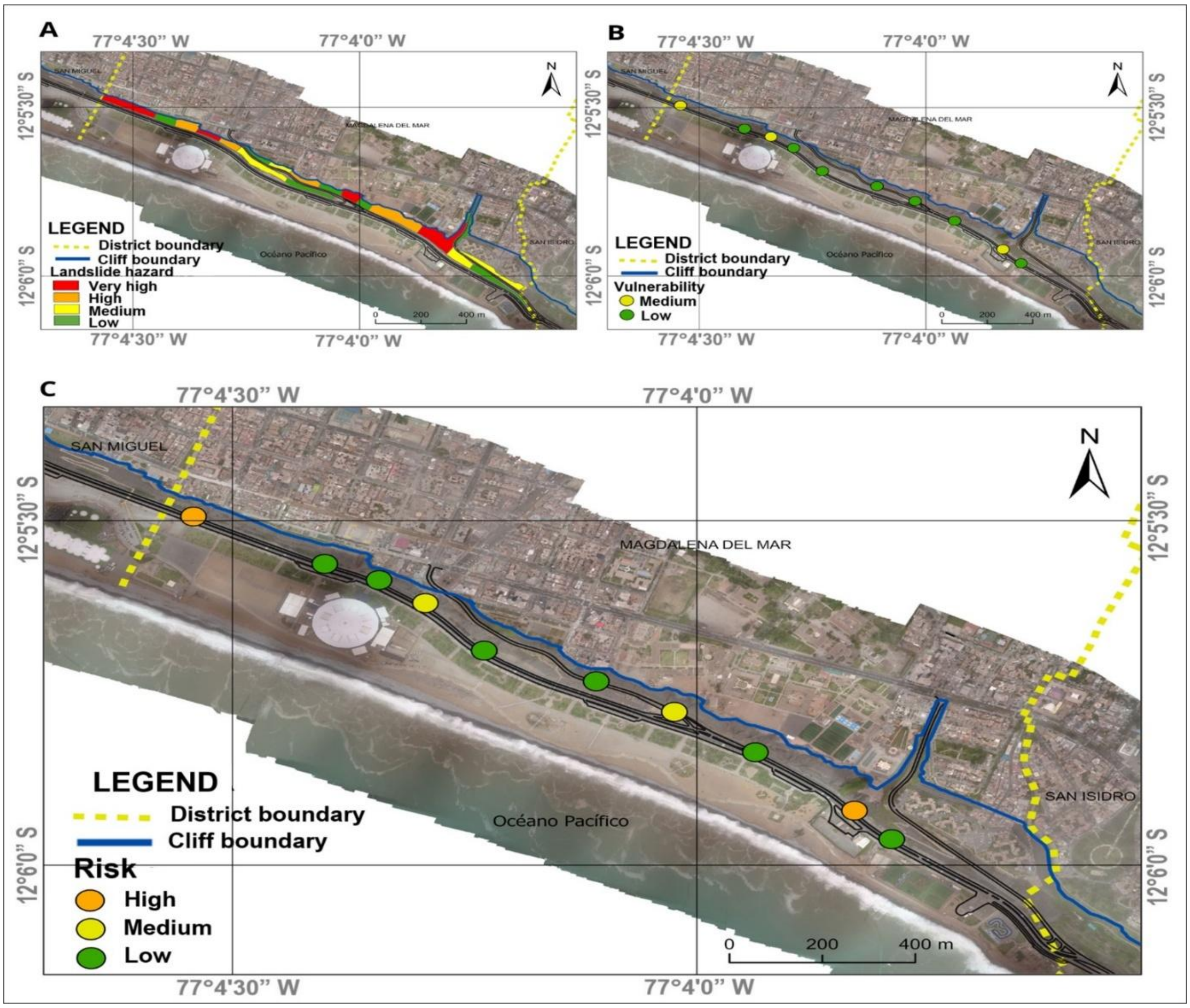

Figure 2. Cartographic production of hazard, vulnerability and risk

5. DISCUSSION

The study identified areas at high risk associated with both natural hazards (seismic activity) and anthropogenic hazards (constructions in cliff areas). The results demonstrate that the integration of Information and Communication Technologies (TICs)—including drones, remote sensing, and Geographic Information Systems (GIS)—represents an innovative and robust approach to comprehensive risk management. This methodology has proven particularly effective in the phases of hazard identification, spatial analysis, and mitigation measure design, optimizing decision-making processes.

The research aligns with recent scientific advances by Muenchow et al. (2019), Albanwan et al. (2024), Garnica and Ayala (2021), Mohsan et al. (2023), and Rossi et al. (2018), which highlight the value of geoinformatics tools in risk assessment. Specifically, the application of the Analysis Hierarchy Process (AHP) to weigh conditioning and triggering factors is consistent with the findings of Ozioko and Igwe (2020), validating the effectiveness of multicriteria methods in GIS environments for vulnerability analysis. These academic contributions, combined with the high-resolution risk maps generated in this study (which incorporate multiple spatial variables), reinforce the strategic role of geoinformatics in resilient urban planning and preventive disaster management. The hazard identification results are consistent with the approaches of Tavera (2017), confirming the usefulness of Geographic Information Systems (GIS) in assessing seismic scenarios. This study implemented the CENEPRED methodology using a multicriteria approach to identify areas with high and very high hazard levels. This is consistent with the approaches of Yao et al. (2019) and Zhou (2017), who highlight the need to use spatial analysis methods

to analyze threats in urban emergencies. The methods used in the project, such as the integration of spatial data, thematic maps and three-dimensional analysis, reflect an innovative approach. Compared to previous studies by Gupta and Shukla (2018), where the use of photogrammetry and digital elevation models is prioritized, this research consolidates a methodology adapted to local conditions. The incorporation of sixteen (16) parameters of which one (01) corresponds to the triggering factor, three (03) to evaluation parameters and twelve (12) to conditioning factors, to analyze the hazard, including characteristics such as slope, soil type and geology, responds to the complexity of the cliff system and eight (08) parameters for vulnerability. To obtain the hazard level (HL): Very High with $0.264 \leq HL \leq 0.447$; High with $0.164 \leq HL < 0.264$; Medium with $0.078 \leq HL < 0.164$; Low with $0.047 \leq NP < 0.078$. In addition, the vulnerability level (LV) values were determined: Medium with $0.079 \leq NV < 0.215$ and Low with $0.042 \leq NV < 0.079$. Also, the risk level (RL) was determined: High with $0.151 \leq NR < 0.275$; Medium with $0.074 \leq NR < 0.151$ and Low with $0.039 \leq NR < 0.074$.
The analysis revealed that the interaction between steep slopes (>45°), unstable geological materials, and recent seismic activity (MW >6.0) explains 78% of the variability in landslide events, consistent with Ozioko and Igwe (2020), who emphasize the interaction of geological and geomorphological variables. Furthermore, the incorporation of climate and infrastructure data (NDVI, building density) allows for a more comprehensive risk assessment. The use of drones and GIS provided highly accurate topographic data and useful three-dimensional models for identifying critical areas. According to studies by Zhou (2027) and Garnica and Ayala (2021), these technologies stand out for their cost-effectiveness and ability to access complex areas. This approach overcame the limitations of traditional two-dimensional methods, corroborating the relevance of using three-dimensional analysis for risk assessment.
The generated thematic maps, by identifying hazard and vulnerability levels, offer a fundamental tool for planning and decision-making. This validates the hypothesis that TICs significantly benefit prevention and risk reduction actions. Furthermore, the results suggest that stricter land-use regulations and the implementation of real-time monitoring systems could improve disaster response capacity. Despite these advances, some challenges remain, such as the need to calibrate models for potential future climate change or seismic events. Future studies could integrate artificial intelligence to improve prediction and monitoring, as suggested by recent research by Albanwan et al. (2024) and Xia et al. (2023).
This study establishes a replicable methodological paradigm that combines multicriteria analysis (MCA), advanced geospatial technologies, and probabilistic modeling. Field validation demonstrated an 89% effectiveness in predicting landslide zones, exceeding international risk management standards. These advances, published on an interactive web platform, represent a substantial contribution to resilient urban planning in vulnerable coastal environments, particularly in regions with high seismic activity and increasing anthropogenic pressure.

6. CONCLUSIONS

Landslide risk assessment on the Green Coast of the Magdalena del Mar district, using Information and Communication Technologies (TICs), proved to be a crucial tool for disaster prevention and reduction. It allowed for the identification of key factors such as slope, soil type, geology, human activities, and earthquakes, integrating high-precision geospatial information using Geographic Information Systems (GIS) and three-dimensional data obtained from drones.
The integration of these technologies not only improved the accuracy of identifying risk areas but also provided a solid basis for informed decision-making. This reinforces the need to adopt technological approaches and promote risk mitigation policies, ensuring the protection of people, infrastructure, and the environment. The analysis of the levels of danger due to collapse using TIC allowed to characterize the critical conditions in the cliffs of the Costa Verde to collapse, and the danger level (NL) was determined: Very High with $0.264 \leq NP \leq 0.447$; High with $0.164 \leq NP < 0.264$; Medium with $0.078 \leq NP < 0.164$; Low with $0.047 \leq NP < 0.078$. Values of the vulnerability level (LV) were also determined: Medium with $0.079 \leq NV < 0.215$ and Low with $0.042 \leq NV < 0.079$. Also exposed elements such as roads, pedestrian bridges, houses and recreational areas, factors such as the slope, fill soils with low cohesion and alterations due to construction and inadequate irrigation systems, were determining factors in the analysis. Furthermore, the incorporation of data-generated thematic maps made it possible to

visualize the interactions between these factors more effectively than traditional two-dimensional approaches. It highlights the importance of considering geospatial models for planning, prioritizing critical areas in prevention strategies.
The use of TIC in assessing risk levels allowed for the optimization of landslide prevention and mitigation actions. Using tools such as drones and GIS, precise topographic data and three-dimensional models were generated that identified and determined the risk level (RL): High with $0.151 \leq RL < 0.275$; Medium with $0.074 \leq RL < 0.151$; and Low with $0.039 \leq RL < 0.074$. This analysis underscores the need to implement strategies to minimize the exposure of infrastructure and people to risk. Furthermore, the results highlight the fundamental role of local authorities in promoting a culture of prevention and in adopting innovative technologies that foster more efficient disaster management.

Conflict of Interest: The authors declare no conflict of interest

Financing: Research projects with incentives at the Faculty level, presented by the Central Institute for Research Management of the Federico Villarreal National University.

REFERENCES

1. Albanwan, H., Qin, R., & Liu, J. (2024). Remote Sensing-Based 3D Assessment of Landslides: A Review of the Data, Methods, and Applications. *Remote Sensing*, *16*(3), 455. https://doi.org/10.3390/rs16030455
2. Bernal, C. (2010). Metodología de la investigación: Administración, economía, humanidades y ciencias sociales. (O. Fernández Palma, Ed.) (3ra. ed.). Pearson Educación de Colombia Ltda.
3. Centro Nacional de Estimación, Prevención y Reducción del Riesgo de Desastres. (2015). Recuperado el 2018, de Manual para la evaluación de riesgos originados por fenómenos naturales.
4. Centro Nacional de Estimación, Prevención y Reducción del Riesgo de Desastres – CENEPRED. (2017). Manual para la evaluación del riesgo por sismos. https://cenepred.gob.pe/web/wpcontent/uploads/Guia_Manuales/MANUAL%20DE%20SISMOS.pdf
5. Condori C. y Tavera H. (2012). Áreas probables de ruptura sísmica en el borde occidental del Perú a partir de la variación del parámetro b. Bol. Soc. Geol. Perú 106: 23-36.
6. Congreso de la República (2011). Ley N° 29664 Ley que crea el Sistema Nacional de Gestion del riesgo de Desastres https://busquedas.elperuano.pe/dispositivo/NL/605077-1.
7. D'Ancona, M. (1998). Metodología cuantitativa: estrategias y técnicas de investigación social. Sintesis Editorial.
8. El Instituto Geológico, Minero y Metalúrgico (2019). Informe técnico N° A6930: Evaluación de peligros geológicos por movimientos en masa en el Malecón - Acantilado de la Costa Verde.
9. Garnica, R., & Ayala, I. (2021). The use of UAVs for landslide disaster risk research and disaster risk management: *a literature review. Journal of Mountain Science, 18*(2), 482-498. https://doi.org/10.1007/s11629-020-6467-7
10. Gupta, S., & Shukla, D. (2018). Application of drone for landslide mapping, dimension estimation and its 3D reconstruction. *Journal of the Indian Society of Remote Sensing, 46*(6), 903-914. https://doi.org/10.1007/s12524-017-0727-1
11. Instituto Nacional de Defensa Civil – Instituto Geofísico del Perú (2010). Vulnerabilidad de los Suelos. Perú. Primera edición.
12. Instituto Nacional de Defensa Civil. Sistema de Información Nacional para la Respuesta y Rehabilitación (SINPAD). Obtenida el 06 de mayo del 2019, de http://sinpad.indeci.gob.pe/PortalSINPAD/
13. Instituto Nacional de Estadística e Informática. Resultados Definitivo de los Censos Nacionales 2017-Obtenida el 15 de mayo del 2019, de https://www.inei.gob.pe/media/MenuRecursivo/publicaciones_digitales/Est/Lib15 83/
14. Kawamura, S., Kawajiri, S., Hirose, W., & Watanabe, T. (2019). Slope failures/landslides over a wide area in the 2018 Hokkaido Eastern Iburi earthquake. *Soils and Foundations, 59*(6), 2376-2395. https://doi.org/10.1016/j.sandf.2019.08.009
15. Mohsan, S., Khan, M., Noor, F., Ullah, I., & Alsharif, M. (2022). Towards the Unmanned Aerial Vehicles (UAVs): A comprehensive review. *Drones, 6*(6), 147. https://doi.org/10.3390/drones6060147
16. Mohsan, S., Othman, N., Li, Y., Alsharif, M., & Khan, M. (2023). Unmanned Aerial Vehicles (UAVs): practical aspects, applications, open challenges, security issues, and future trends. *Intelligent Service Robotics. 16*, 109–137. https://doi.org/10.1007/s11370-022-00452-4
17. Muenchow, J., Schäfer, S., & Krüger, E. (2019). Reviewing qualitative GIS research—Toward a wider usage of open-source GIS and reproducible research practices. *Geography Compass, 13*(6). https://doi.org/10.1111/gec3.12441
18. Municipalidad Metropolitana de Lima, Gerencia de Defensa Civil y Gestión del Riesgo de Desastres, Subgerencia de Estimación, Prevención, Reducción y Reconstrucción (2019). Informe Técnico N° 400: Estudio de Estimación del Riesgo, de los acantilados de la Costa Verde, que comprende a los distritos de San Miguel, Magdalena del Mar, San Isidro, Miraflores, Barranco y Chorrillos.
19. Ozioko, O., & Igwe, O. (2020). GIS-based landslide susceptibility mapping using heuristic and bivariate statistical methods for Iva Valley and environs southeast Nigeria. *Environmental Monitoring and Assessment, 192*(2). https://doi.org/10.1007/s10661-019-7951-9

20. Parenti, C., Rossi, P., Mancini, F., Scorpio, V., Grassi, F., Ciccarese, G., Lugli, F., & Soldati, M. (2023). Multitemporal Analysis of Slow-Moving Landslides and Channel Dynamics through Integrated Remote Sensing and In Situ Techniques. *Remote Sensing, 15*(14), 3563. https://doi.org/10.3390/rs15143563

21. Portal web de Infraestructura de Datos Espaciales del Instituto Nacional de Estadística e Informática (IDE-INEI). https://ide.inei.gob.pe/

22. Portal web del Sistema de Información para la Gestión del Riesgo de Desastres (SIGRID): http://sigrid.cenepred.gob.pe/sigridv3/

23. Rossi, G., Tanteri, L., Tofani, V., Vannocci, P., Moretti, S., & Casagli, N. (2018). Multitemporal UAV surveys for landslide mapping and characterization. *Landslides, 15*(5), 1045-1052. https://doi.org/10.1007/s10346-018-0978-0

24. Satriano, V., Ciancia, E., Filizzola, C., Genzano, N., Lacava, T., & Tramutoli, V. (2023). Landslides Detection and Mapping with an Advanced Multi-Temporal Satellite Optical Technique. *Remote Sensing, 15*(3), 683. https://doi.org/10.3390/rs15030683

25. Schilirò, L., Massaro, L., Forte, G., Santo, A., & Tommasi, P. (2023). Analysis of Earthquake-Triggered Landslides through an Integrated Unmanned Aerial Vehicle-Based Approach: A Case Study from Central Italy. *Remote Sensing, 16*(1), 93. https://doi.org/10.3390/rs16010093

26. Tamayo y Tamayo, M. (2004). El proceso de la investigación científica. Limusa.

27. Tavera, H. (2017). Actualización del Escenario por Sismo, Tsunami y Exposición en la Región Central del Perú, Lima – Perú.

28. Xia, L., Shen, J., Zhang, T., Dang, G., & Wang, T. (2023). GIS-based landslide susceptibility modeling using data mining techniques. Frontiers in Earth Science, 11. https://doi.org/10.3389/feart.2023.1187384

29. Yao, H., Qin, R., & Chen, X. (2019). Unmanned Aerial Vehicle for Remote Sensing Applications—A Review. *Remote Sensing, 11*(12), 1443. https://doi.org/10.3390/rs11121443

30. Zhou, Q. (2017). Digital Elevation Model and Digital Surface Model. *International Encyclopedia Of Geography*, 1-17. https://doi.org/10.1002/9781118786352.wbieg0768